Formation and electronic properties of BC_3 single-wall nanotubes upon boron substitution of carbon nanotubes

G. G. Fuentes, E. Borowiak-Palen, M. Knupfer, T. Pichler, and J. Fink
Leibnitz-Institute für Festkörper- und Werkstoffforschung Dresden, P.O. Box 270016, D-01171 Dresden, Germany

L. Wirtz and A. Rubio
Department of Material Physics, University of the Basque Country, Centro Mixto CSIC-UPV, and Donostia International Physics Center, Po. Manuel de Lardizabal 4, 20018 San Sebastián, Spain

(Received 17 November 2003; revised manuscript received 3 February 2004; published 10 June 2004)

We report a detailed experimental and theoretical study on the electronic and optical properties of highly boron-substituted (up to 15 at.%) single-wall carbon nanotubes. Core-level electron energy-loss spectroscopy reveals that the boron incorporates into the lattice structure of the tubes, transferring $\sim 1/2$ hole per boron atom into the carbon derived unoccupied density of states. The charge transfer and the calculated Fermi-energy shift in the doped nanotubes evidence that a simple rigid-band model can be ruled out and that additional effects such as charge localization and doping induced band-structure changes play an important role at this high doping levels. In optical absorption a new peak appears at 0.4 eV which is independent of the doping level. Compared to the results from a series of *ab initio* calculations our results support the selective doping of semiconducting nanotubes and the formation of BC_3 nanotubes instead of a homogeneous random boron substitution.

DOI: 10.1103/PhysRevB.69.245403 PACS number(s): 78.30.−j, 61.46.+w, 63.20.Dj

I. INTRODUCTION

Tuning the electronic properties of single-wall carbon nanotubes (SWCNT) (Refs. 1 and 2) by substitution of carbon by heteroatoms represents one of the most promising routes to extend their application possibilities.[3] It also opens a series of basic scientific questions regarding, e.g., charge transfer between B and C atoms, band-structure change, and charge-carrier localization. Recent studies[4–7] were mainly focused on boron and nitrogen doping of multiwalled carbon nanotubes (MWCNT). They have already successfully achieved boron or nitrogen incorporation by different procedures. Recently, Golberg *et al.*[6] reported the B and N substitution of SWCNT by a substitution reaction at high temperatures.

Despite the importance of these one-dimensional (1D) heteronanostructures, only very few experimental studies have been devoted to their electronic properties. The electronic structure of multiwall boron doped nanotubes was studied on a local scale by scanning tunneling spectroscopy (STS).[8] Spectroscopic studies of the electronic properties of single-wall heteronanotubes are still missing to our knowledge.

In theory, the role of the B or N atoms in the electronic structure of modified sp^2-hybridized carbon networks has been treated using different approaches. Mele and Ritsko[9] used a tight-binding approach to calculate the core exciton spectrum of graphite and showed that the changes induced by low B substitution (0.5 at.%) can be explained by a rigid-band shift model, i.e., assuming that the Fermi level is shifted downwards due to the missing π electrons from the boron atoms while the valence-band structure remains otherwise undisturbed. Yi and Bernholc[18] calculated *ab initio* for a (10,0) nanotube with 1.25 at.% B substitution the formation of a shallow acceptor state at 0.16 eV above the Fermi level. Band-structure calculations of hypothetical tubule forms of hexagonal BC_3 predicted that these tubes form as likely as carbon and BN nanotubes and have a minimum energy gap of about 0.2 eV.[10] Carroll *et al.*[8] proposed that B substitution of CNT's leads to the formation of BC_3 nanodomains inserted in the 1D nanotube structure, giving rise to an acceptor state 0.4 eV below the Fermi level due to the realignment of this superstructure with the graphitic one. Lammert *et al.*[19] showed that under doping with boron and nitrogen, the microscopic doping inhomogeneity of carbon nanotubes is larger than in normal semiconductors leading to charge fluctuations that can be used to design nanoscale devices (diode behavior).

In this paper we report on a spectroscopic study of highly B-doped SWCNT (B-SWCNT) using high-resolution nonspatially resolved electron energy-loss spectroscopy and optical spectroscopy. The spectroscopic response is then interpreted with the help of *ab initio* band-structure calculations using density-functional theory in the local-density approximation (DFT-LDA). Our results evidence the preferential doping of semiconducting SWCNT and the formation of BC_3 single-wall nanotubes in boron substituted SWCNT samples.

II. EXPERIMENTAL RESULTS

SWCNT with a mean diameter of 1.23 nm were produced by the laser ablation technique.[11] Boron doping with an averaged substitution level of $\sim$15 at.% was achieved by a substitution reaction in an NH_3 atmosphere.[12] Transmission electron microscopy (TEM) characterization after the substitution reaction revealed the presence of high-purity nanotube bundles with a homogeneous diameter distribution. Transmission electron microscopy electron energy-loss spectros-

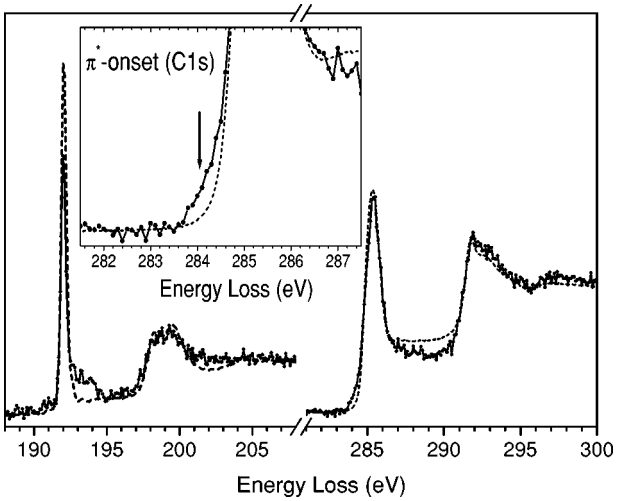

FIG. 1. B1*s* (left) and C1*s* (right) EELS spectra of boron doped SWCNT. Right inset: Expanded scale to focus on the $C1s \rightarrow \pi^*$ excitation onset. The dashed lines represent reference spectra from the B1*s* excitation edge of MWBNNT (Ref. 14) and the C1*s* edge of pristine SWCNT, respectively. The spectra are normalized to the respective $1s \rightarrow \sigma^*$ excitation peaks at 199 eV and 292 eV for B and C, respectively.

copy mode (TEM-EELS) analysis with 10 nm beam size showed that locally the substitution level is up to 20 at.%. Films of 100 nm effective thickness were prepared as described elsewhere.[12] Optical-absorption spectra were measured with a resolution of 0.25 meV. Core-level excitation spectra were collected in a purpose built high-resolution EELS spectrometer described elsewhere.[13] The energy resolution was set to 200 meV. The bulk sensitive EELS spectroscopy indicated an averaged boron atomic concentration of about 15 at.%, in agreement with our previous local TEM-EELS analysis.[12] In addition, both TEM and bulk sensitive EELS revealed nitrogen concentrations always below the sensitivity of the method (1.5 at.%).

An overview over the B1*s*, C1*s*, and N1*s* core-level excitation spectra of B-SWCNT confirmed the sp^2-hybridized bonding environment. This fact and the absence of the N1*s* signal as compared to C1*s* and B1*s* are in good agreement to the local analysis by TEM-EELS (Ref. 12) and show the efficiency of the substitution process. For a more detailed analysis the B1*s* and C1*s* core excitation edges of the B-SWCNT (solid) and the reference B1*s* and C1*s* spectra from multiwalled boron nitride nanotubes (MWBNNT) (Ref. 14) and SWCNT, respectively, (dashed) are shown in Fig. 1. The inset in Fig. 1 represents an expanded scale focusing on the threshold of the π^* resonance of the C1*s* edges of B-SWCNT (solid) and pristine SWCNT (dashed). Essentially, the excitation spectra represent in a first approximation the projected matrix element weighted density of unoccupied states of each atom participating in the band structure. In addition, final-state effects of the remaining 1*s* core hole lead to a strong redistribution of the spectral weight. For instance, it is well established that in the case of 1*s* excitation edges of pristine SWCNT (Ref. 17) and MWBNT (Ref. 14) both the π^* and σ^* onsets are dominated by spectral weight resulting from the influence of the core-hole. Thus, assuming a similar interaction between the excited electron and the core-hole in B-SWCNT, one can expect that the π^* resonances related to the density-of-states (DOS) singularities of the different types of SWCNT are washed out, resulting in the broad π^* resonances. Nevertheless, the edges can be used to study some details in the electronic structure.

The B1*s* spectrum of B-SWCNT shows an intense peak at 192 eV assigned to the $1s \rightarrow \pi^*$ resonance and a less intense double peak at 199 eV due to the $1s \rightarrow \sigma^*$ resonance. The small shoulder at 194 eV can be assigned to residual B_2O_3 from the precursor material. The C1*s* spectrum of B-SWCNT shows the excitonic $1s \rightarrow \pi^*$ absorption at 285.3 eV, as in the case of the SWCNT reference, and the corresponding $1s \rightarrow \sigma^*$ absorption at 292 eV. The spectral shape of the $C1s \rightarrow \pi^*$ and the $C1s \rightarrow \sigma^*$ resonances of the B-SWCNT resemble quite well those of the pure material, indicating that the boron substitution does not alter the chemical environment of the carbon atoms of the tube significantly.

The comparison of the B1*s* spectrum of the B-SWCNT with that of the BN nanotubes indicates that the chemical environment of boron is rather similar to that expected for an sp^2-hybridized environment, as it is also characteristic of *h*-BN, which constitutes clear experimental confirmation that the boron atoms are incorporated into the hexagonal lattice structure of the nanotube, in good agreement with the theoretical predictions.[8,18,19] The area below the π^* resonance gives a measure of the charge transfer and bonding environment. We observe that the B1*s* π^* peak is about 13% lower in the B-SWCNT than in the MWBNNT, which shows that there is a different charge distribution within the B-C bonds which results in a higher electron density at the boron site. Turning back to the C1*s* excitation spectra, the inset of Fig. 1 provides evidence for the appearance of additional unoccupied states of carbon character in the electronic structure of the B-SWCNT, as clearly shown by the low-energy shoulder observed at the C1*s* excitation threshold and indicated by the arrow. The energy position of this feature can be roughly estimated around 0.7 eV below the corresponding $C1s \rightarrow \pi^*$ threshold of the pure SWCNT. In analogy to *p*-type doping in graphite intercalation compounds,[15] the presence of this doping-induced feature reflects that the Fermi level of the B-SWCNT shifts to lower energies with respect to that of the SWCNT. Although the corresponding total shift of the Fermi level from a comparison of both spectra alone can be complicated by additional effects such as different excitonic effects or the mixture of semiconducting and metallic tubes, the observed shift by 0.7 eV of the C1*s* excitation onset establishes a good estimate for the Fermi-level shift assuming a rigid-band shift without strong changes of the SWCNT band structure as it is observed, for instance, for $FeCl_3$ intercalated SWCNT.[16] Hence, the shift in the onset of spectral weight and the increase of the response of the π^* resonance confirms that there exists a charge transfer from the boron atom to the C-derived bands. However, the analysis of Fig. 1 indicates that the shoulder is only about 6% of the total area, suggesting a charge transfer to carbon derived states of $\sim 1/2$ holes per boron atom which is lower than the estimation by Mele *et al.*[9] for B-doped graphite ($\sim$0.8 holes per B). This difference in the charge transfer also means a different charge

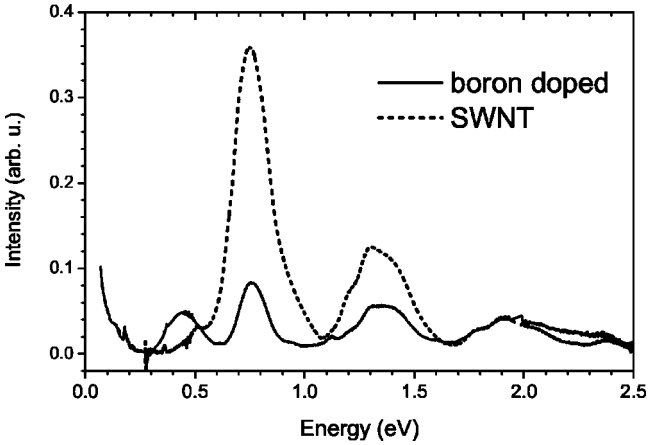

FIG. 2. Optical-absorption spectra of boron doped SWCNT (solid) and pristine SWCNT (dashed).

delocalization around the B site and therefore is a hint for a different bonding environment in the B-SWCNT as compared to B-doped graphite. In other words, the boron doping of SWCNT cannot be solely explained within the framework of a simple rigid-band model and additional changes in the nanotube band structure have to be taken into account.

Information about the dielectric function and hence the matrix element weighted joint DOS can be retrieved from optical-absorption spectroscopy. The normalized optical-absorption response of both B-SWCNT and pristine SWCNT are shown in Fig. 2 between 0.05 eV and 2.5 eV. In order to determine the relative peak intensities the spectra were normalized and the background was subtracted as described in detail previously.[23] The spectrum of pristine SWCNT is dominated by two strong absorptions at 0.75 eV and 1.35 eV attributed to the two first allowed optical transitions between the Van Hove singularities (vHS) of the semiconducting SWCNT (at an average tube radius of 14 Å) and a less intense feature at 1.93 eV corresponding to the first transition in metallic SWCNT. Essentially, the spectrum of B-SWCNT shows the same absorption peaks as the pure SWCNT but with an overall reduced intensity for the peaks originating from semiconducting tubes and with the same intensity in the case of the peak which corresponds to the metallic ones. Especially the peak at 0.75 eV which was successfully used to determine the yield in pristine nanotube samples[11] is reduced to about 20% of its intensity. The fact that the metallic tubes are less affected by the substitution reaction than the semiconducting ones is consistent with calculations by Blase *et al.*[21] who reported that the growth yield of metallic B-SWCNT is much lower than that of the semiconducting tubes. This fact suggests that our substitution method leads to a preferential B substitution of semiconducting tubes. Nevertheless, further studies sensitive to the electronic properties of either metallic or semiconducting tubes should be carried out in order to understand the observed differences. Interestingly, a new absorption peak shows up at about 0.4 eV in the case of the B-SWCNT which we assign to an optical excitation from the valence band into a new unoccupied acceptor-like band induced by the boron substitution. Additional experiments using samples with a lower substitution level of about 5 at.% of B reveal that the position of this new absorption peak remains basically unchanged, whereas the spectral weight is strongly reduced.[22]

III. BAND-STRUCTURE CALCULATIONS AND INTERPRETATION OF EXPERIMENTAL RESULTS

In order to elucidate the observed effects of B substitution on the electronic properties of SWCNT, we have performed a series of DFT-LDA band-structure calculations.[25,26]We use the example of a semiconducting (16,0) tube with a diameter of 12.5 Å which is close to the mean diameter of the SWCNT sample used in the experiment. In order to elucidate the effect of the boron concentration on the electronic structure, we present in Fig. 3 the band structure and the density of states (DOS) with different degrees of B substitution. We have chosen a regular periodic ordering of the boron atoms (see insets) in order to keep the unit cell small and the calculations feasible. For the undoped tube [Fig. 3(a)], our calculations reproduce the well-known result that the one-dimensional DOS (within DFT–LDA or tight-binding models) is symmetric around the band gap for the first and second vHS. Beyond this small energy regime around the band gap, asymmetries arise due to the mixing of p and s orbitals. Doping of the tubes leads to a lowering of the Fermi level into the valence band of the undoped tubes [Figs. 3(b)–3(d)]. Clearly, the stronger the doping, the stronger is also the shift of the Fermi level. For a substitution level of 25%, the level shift reaches 2.2 eV. The rigid-band shift model (shift of the Fermi level without altering the band structure) clearly breaks down for strong concentrations: Above the highest occupied state of the undoped tube new bands are formed. This corresponds to the formation of an acceptor level (unoccupied state within the band gap) in semiconductors with very low dopant concentration. However, in the present case, due to the strong concentration of boron atoms, the acceptor levels hybridize with the carbon levels and form strongly dispersive "acceptor bands," i.e., new bands that are unoccupied due to the lower number of valence electrons of the boron atoms. Correspondingly, in the DOS, new unoccupied vHS appear giving rise to additional possibilities for electronic excitations.

We expect that the additional peak at 0.4 eV in the absorption spectrum (Fig. 2) is due to electron excitation from the occupied valence states into one of these acceptor bands. Indeed, the joint DOS (divided by E^2) in Fig. 3 display peaks in the energy region between 0.2 and 0.6 eV. The exact position of the additional peaks is, however, strongly dependent on the doping concentration. Furthermore, calculations with the same degree of substitution but with different arrangement of the boron atoms show large differences in the formation of acceptor bands.[27] In particular, self-consistent tight-binding calculations with a pseudorandom ordering of boron atoms in a large supercell containing several hundred atoms display a smearing out of the vHS pattern.[27] In that case, a quasicontinuous set of electronic transitions would completely wash out the optical-absorption spectrum. Hence, these results do not at all fit to the experimental observations. Due to the strong dependence of the band structure on the

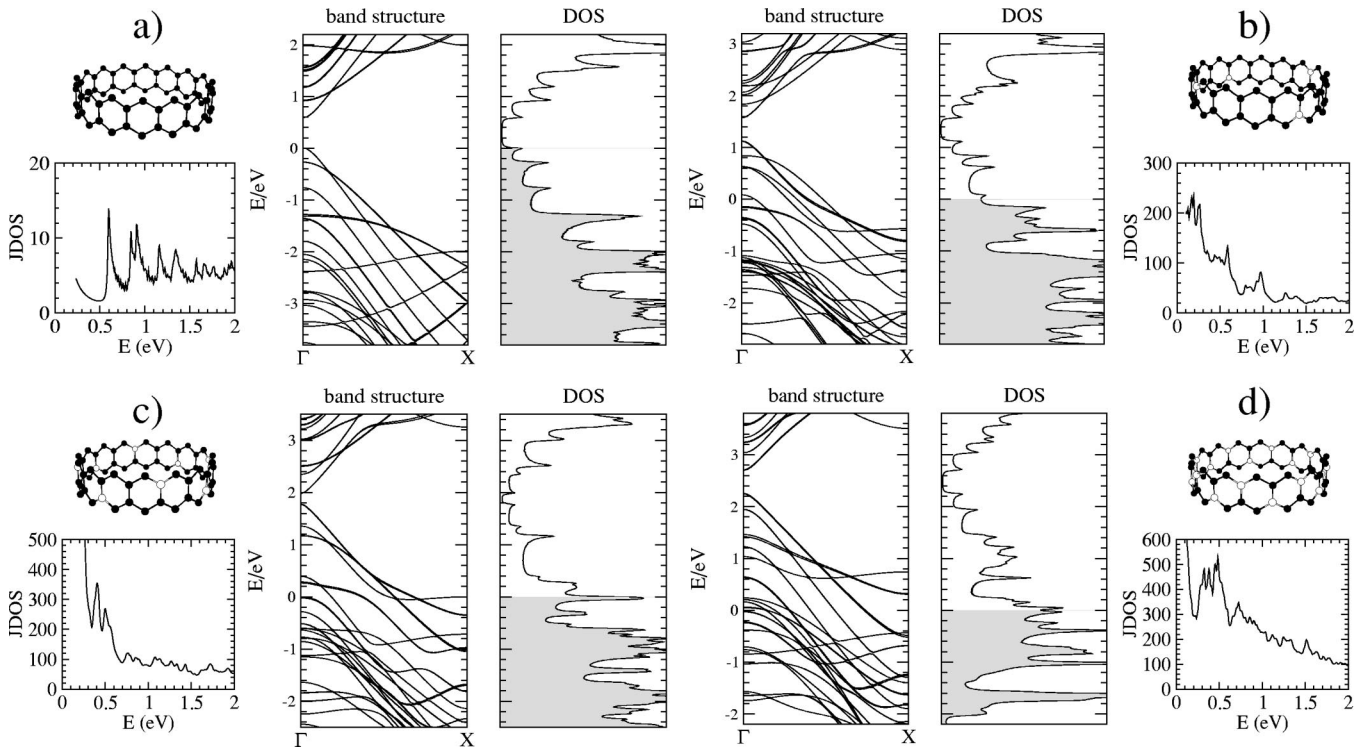

FIG. 3. Band structure, DOS and joint DOS divided by E^2 of a C(16,0) tube with (a) 0%, (b) 6.25%, (c) 12.5%, and (d) 25% boron doping. Zero energy denotes the Fermi energy. Filled states are indicated by gray shadowing. Also displayed are the corresponding unit cells (C atoms black, B atoms white).

degree of substitution and the particular arrangement of the boron atoms, we conclude that the observed optical-absorption spectra in Fig. 2 can be best explained with the assumption that only one particular kind of boron substituted tubes is formed in our experiment. Only a subset of tubes from the sample are doped (with a corresponding higher concentration) while the other tubes remain almost pure carbon tubes. This explains the stable peak positions in the spectra. The peaks at 0.7 and 1.4 eV are due to the transitions between first and second vHS in the pure semiconducting carbon tubes. In strongly B-doped samples they should disappear because of the Fermi-level lowering. However, the survival of a large fraction of pure carbon tubes explains the survival of these peaks and the decreasing intensity with increasing fraction of boron atoms in the sample. The unchanged intensity of the peak at 1.9 eV is consistent with the assumption that metallic tubes are less susceptible for Boron substitution.[21]

We assume the formation of BC_3 tubes in our samples (25% substitution) which is consistent with the average degree of substitution (up to 15%) in our sample. The BC_3 structure has been shown to be relatively stable (with respect to other arrangements) both for the sheet[28] and for single-wall tubes.[10] The relative stability is likely connected with the fact that these tubes are semiconducting with a gap between the occupied π orbitals and the π orbitals which are unoccupied due to the electron deficiency.

In Figs. 4(a) and 4(b) we present the band structure and DOS of a $BC_3(3,3)$ tube.[29] The tube displays a band gap of 0.4 eV between occupied and unoccupied π orbitals in agreement with the tight-binding band structure of Ref. 10. The joint density of states [divided by E^2 in Fig. 4(c)] displays accordingly the first vertical transition at about 0.4 eV in very good agreement with the observed absorption peak. We note that calculations of the optical response[30] [dashed line in Fig. 4(c)] of such a perfect BC_3 nanotube show that the first optically allowed transition is at about 1.8 eV (very

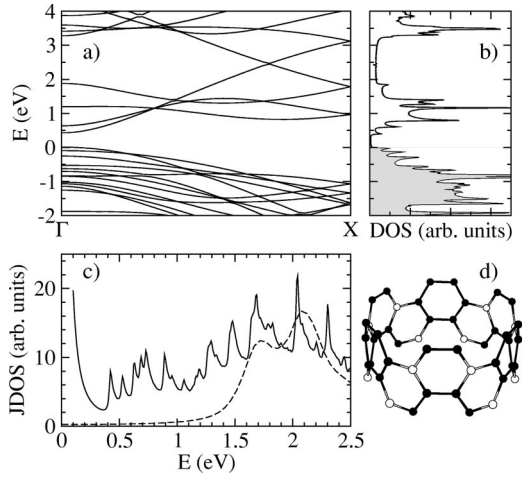

FIG. 4. (a) Band structure of $BC_3(3,3)$ nanotube (Fermi energy at 0 eV). (b) Density of states (filled states shadowed with gray). (c) Joint density of states divided by E^2 (solid line) and calculated optical absorption (dashed line) of a perfect infinite $BC_3(3,3)$ tube with light polarization along the tube axis. (d) Sketch of the unit cell.

similar to hexagonal BC_3 sheets). The fact that we observe a peak at 0.4 eV can be explained by symmetry breaking due to defects which are created during the substitution process.

The formation of BC_3 SWNT during the substitution process also explains the higher local boron concentration observed on selected TEM spots and the remaining optical response of the pristine SWCNT. Furthermore, different concentrations of BC_3 tubes at different substitution levels also explain why the acceptor-induced absorption peak does not shift by changing the doping level between 5% and 15%. As a final consistency check we can estimate the upper limit for the substitution level from the decrease of the first absorption peaks of the semiconducting and metallic SWCNT, assuming that all of the remaining response is from not substituted nanotubes.[31] Since BC_3 corresponds to 25% B substitution and from the decrease of the SWCNT intensity about 80% of the semiconducting SWCNT and within the experimental error none of the metallic tubes are doped we end up with an average doping level of about 13% in very good agreement with the value derived from the core-level excitation measurements. Compared to boron-doped silicon or graphite, there are distinct differences since the dopant concentration in our case is orders of magnitude higher than in classical semiconductor physics. Due to our high doping level a new stable hexagonal BC_3 structure is formed where the boron levels hybridize with the carbon levels and form strongly dispersive acceptor bands.

IV. CONCLUSION

We have studied the electronic properties of highly boron doped SWCNT by bulk sensitive spectroscopies and LDA band-structure calculations. Core-level excitation spectroscopy of the B1*s* and C1*s* edges revealed that the boron atoms substitute carbon atoms in the tube lattice keeping an sp^2-like bond with their nearest C neighbor atoms. The effective charge transfer to the C derived conduction bands is about 0.5 holes per substituted B atom. Optical absorption indicates the formation of an acceptorlike band in the band structure of the semiconducting tubes. This is nicely confirmed by *ab initio* calculations of the electronic structure of a BC_3 SWNT. The electronic structure characteristic of the B-SWCNT is influenced by a strong hybridization of the B and C valence orbitals. Our results show that a simple rigid-band model as has been applied previously to intercalated SWCNT is not sufficient to explain the changes in the electronic properties of highly doped B-SWCNT and a new type of a highly defective BC_3 SWNT with new electronic properties is observed.

ACKNOWLEDGMENT

We acknowledge financial support from the EU: IST Project SATURN and Research Training Network COMELCAN (Grant No. HPRN-CT-2000-00167), and from the DFG (Project PI 440). G.G.F. thanks for financial support by the EU Marie Curie programm. L.W. and A.R. acknowledge additional support by Spanish MCyT (Grant Nos. MAT2001-0946 and MAT2002-04499) and by the University of the Basque Country (Grant No. 9/UPV 00206.215-13639/2001). The authors are grateful to K. Müller for the technical assistance and O. Jost for delivering of as-produced SWCNT raw material. We thank A. Marini for making available his code SELF.

[1] S. Iijima, Nature (London) **354**, 56 (1991).
[2] T. W. Ebbesen, Phys. Today **49** (26), 26 (1996).
[3] N. Hamada, S. I. Sawada, and A. Oshiyama, Phys. Rev. Lett. **68**, 1579 (1992).
[4] Ph. Redlich, J. Loeffler, P. M. Ajayan, J. Bill, F. Aldinger, and M. Rühle, Chem. Phys. Lett. **260**, 465 (1996).
[5] J. Yu, X. D. Bai, J. Ahn, S. F. Yoon, and E. G. Wang. Chem. Phys. Lett. **323**, 529 (2000).
[6] D. Golberg, Y. Bando, W. Han, K. Kurashima, and T. Sato, Chem. Phys. Lett. **308**, 337 (1999).
[7] W. Han, Y. Bando, K. Kurashima, and T. Sato, Chem. Phys. Lett. **299**, 368 (1999).
[8] D. L. Carroll, Ph. Redlich, X. Blase, J.-C. Charlier, S. Curran, P. M. Ajayan, S. Roth, and M. Ruhle, Phys. Rev. Lett. **81**, 2332 (1998).
[9] E. J. Mele and J. J. Ritsko, Phys. Rev. B **24**, 1000 (1981).
[10] Y. Miyamoto, A. Rubio, S. G. Louie, and M. L. Cohen, Phys. Rev. B **50**, 18360 (1994).
[11] O. Jost, A. A. Gorbunov, W. Pompe, T. Pichler, R. Friedlein, M. Knupfer, M. Reibold, H.-D. Bauer, L. Dunsch, M. S. Golden, and J. Fink, Appl. Phys. Lett. **75**, 2217 (1999).
[12] E. Borowiak-Palen, T. Pichler, A. Graff, R. J. Kalenczuk, M. Knupfer, and J. Fink, Chem. Phys. Lett. **387**, 516 (2003).
[13] J. Fink, Adv. Electron. Electron Phys. **75**, 121 (1989) and references therein.
[14] G. G. Fuentes, E. Borowiak-Palen, T. Pichler, X. Liu, A. Graff, G. Behr, R. J. Kalenczuk, M. Knupfer, and J. Fink, Phys. Rev. B **67**, 035429 (2003).
[15] E. J. Mele and J. J. Ritsko, Phys. Rev. Lett. **43**, 68 (1979).
[16] T. Pichler, X. Liu, M. Knupfer, and J. Fink, New J. Phys. **5**, 23.1 (2003).
[17] T. Pichler, M. Sing, M. Knupfer, M. S. Golden, and J. Fink, Solid State Commun. **109**, 721 (1999).
[18] J.-Y. Yi and J. Bernholc, Phys. Rev. B **47**, 1708 (1993).
[19] P. E. Lammert, V. H. Crespi, and A. Rubio, Phys. Rev. Lett. **87**, 136402 (2001).
[20] K. Liu, Ph. Avouris, R. Martel, and W. K. Hsu, Phys. Rev. B **63**, 161404(R) (2001).
[21] X. Blase, J.-C. Charlier, A. DeVita, R. Car, Ph. Redlich, M. Terrones,W. K. Hsu, H. Terrones, D. L. Carroll, and P. M. Ajayan, Phys. Rev. Lett. **83**, 5078 (1999).
[22] E. Borowiak-Palen, T. Pichler, A. Graff, R. J. Kalenczuk, M. Knupfer, and J. Fink, Carbon **42**, 1123 (2004).
[23] X. Liu, T. Pichler, M. Knupfer, M. S. Golden, J. Fink, H. Kataura, and Y. Achiba, Phys. Rev. B **66**, 045411 (2002).
[24] The *ab initio* calculations have been performed with the code

ABINIT abinit1, abinit2. The wave functions of the valence electrons are expanded in plane waves with an energy cutoff at 50 Ry. The core electrons are simulated by Troullier-Martins pseudopotentials. A supercell geometry is employed with a large intertube distance (10 a.u.) in order to minimize the overlap of wave functions of neighboring tubes. The density is calculated self-consistently using a sampling of eight k points for the (quasi-one-dimensional) first Brillouin zone of the tubes. A non-self-consistent calculation yields the energies of occupied and unoccupied states on a grid of 50 k points.

[25] X. Gonze, J.-M. Beuken, R. Caracas, F. Detraux, M. Fuchs, G.-M. Rignanese, L. Sindic, M. Verstraete, G. Zerah, F. Jollet, M. Torrent, A. Roy, M. Mikami, Ph. Ghosez, J.-Y. Raty, and D. C. Allan, Comput. Mater. Sci. **25**, 478 (2002).

[26] The ABINIT code is a common project of the Université Catholique de Louvain, Corning Incorporated, and other contributors (URL http://www.abinit.org).

[27] L. Wirtz and A. Rubio, in *Molecular Nanostructures: XVII International Winter-School/Euroconference on Electronic Properties of Novel Materials*, edited by H. Kuzmany, J. Fink, M. Mehring, and S. Roth, AIP Conf. Proc. No. 685 (AIP, New York, 2003), p. 402.

[28] D. Tománek, R. M. Wentzcovitch, S. G. Louie, and M. L. Cohen, Phys. Rev. B **37**, 3134 (1988).

[29] $BC_3(3,3)$ is the notation of Ref. 10 and corresponds to a B-doped C(6,6) tube with the periodic arrangement of boron atoms as depicted in Fig. 4(d). Note that the unit cell is twice as large as the C(6,6) unit cell. For this reason we have chosen an armchair tube which is metallic in the undoped case. However, the metallicity of the undoped tube does not matter for the present investigation, because both metallic and semiconducting carbon tubes become semiconducting in the BC_3 doping case. We have chosen the $BC_3(3,3)$ tube because it has a sufficiently large diameter such that the DOS around the band gap is already converged while it is still small enough for the *ab initio* calculation of band structure and optical absorption.

[30] The calculation of the optical spectrum has been performed with the code SELF written by A. Marini. We use the random-phase approximation (RPA). The light is polarized along the tube axis. (The first absorption peak for vertically polarized light is at 2.1 eV).

[31] The intensity of the optically allowed E_{11} transition is a direct measure to the SWCNT abundance (see also Ref. 11). Since our sample consists of BC_3 nanotubes and unsubstituted SWCNT this transition provides a measure of the remaining fraction of SWCNT in the transformed sample. We are aware of the fact that the optical response from the BC_3 nanotubes in this energy range could complicate the analysis. However, since the absorption peaks below about 2 eV are only optically allowed by symmetry breaking the sheer number of optically allowed transitions only contributes to the broad background and not to the individual SWCNT derived absorption peaks.